Supplement to "Cell-specific imputation of drug connectivity mapping with incomplete data"

D. Sapashnik, R. Newman, C.M. Pietras, F. Qu, L. Kofman, S. Boudreau, I. Fried, D.K. Slonim

May 11, 2021

Contents:

Cancer	**Primary**
MCF7, HT29, A375, PC3, A549, HCC515 ,	NPC
VCAP, HEPG2, HELA, YAPC, U937, LOVO,	SKB
SNUC4, SKMEL1, RMUGS, HCC15, HEC108, CORL23,	PHH
A673, NCIH596, TYKNU, SW948, SW620, SNU1040,	NEU
SNGM, SKMEL28, OV7, RKO, NCIH508, H1299,	NPC.TAK
AGS, EFO27, SW480, HCT116, JHUEM2, MDST8,	CD34
NCIH2073, COV644, DV90, RMGI, SKLU1, HT115,	SKL
WSUDLCL2, PL21, NCIH1836, NCIH1694, SNUC5, CL34,	NPC.CAS9
THP1, SKM1, T3M10, NOMO1, BT20, HS578T,	SKL.C
MDAMB231, SKBR3, HUH7, JURKAT, LNCAP, HL60	MNEU.E
Immortalized	**Stem Cell**
HA1E	ASC
HME1	FIBRNPC
MCF10A	ASC.C
HUVEC	HUES3
NKDBA	
HEK293T	

Table 1: Cells Types and Cells in Sparse Data Set.

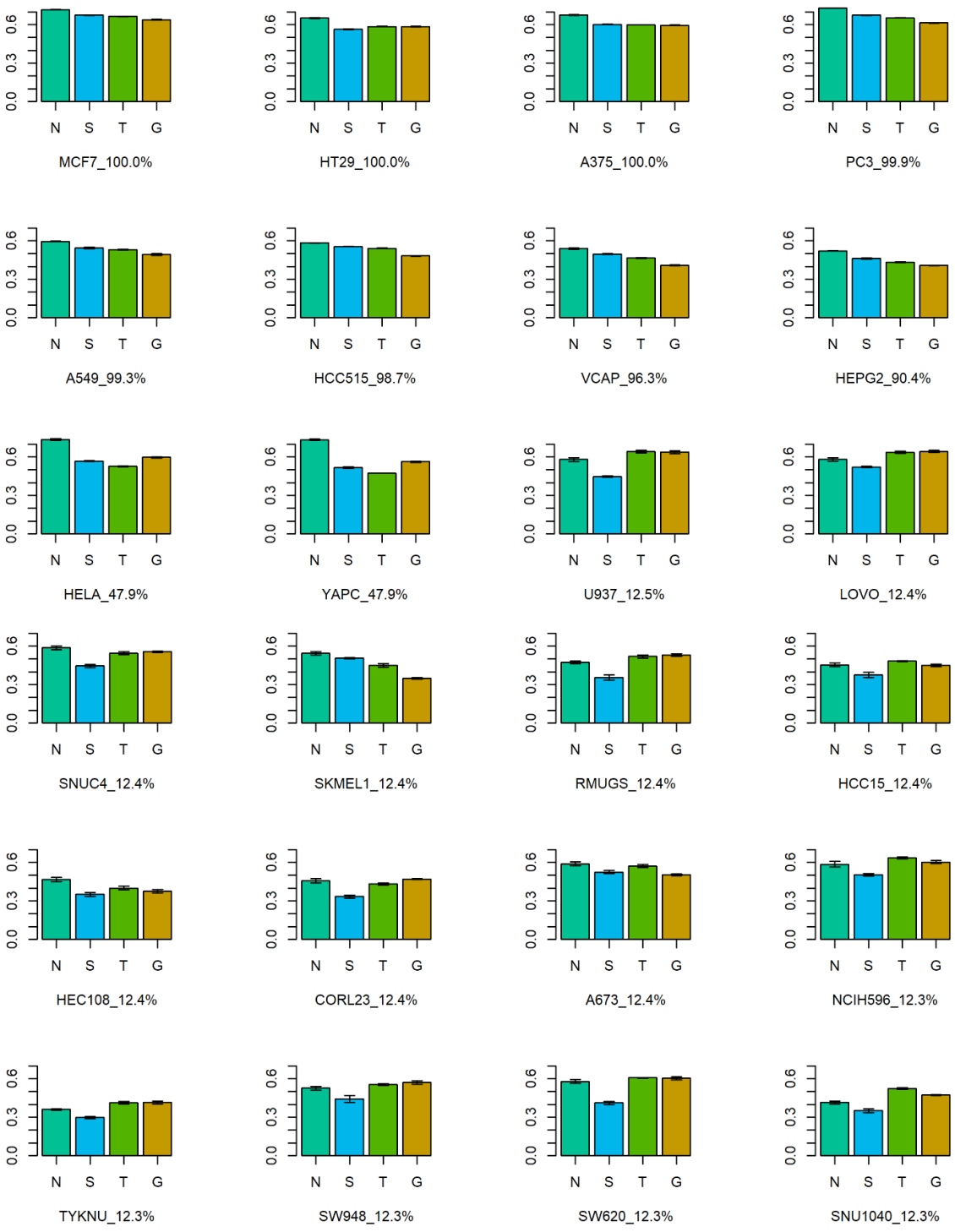
0.0 0.3 0.6
N S T G
MCF7_100.0%
HT29_100.0%
A375_100.0%
PC3_99.9%
A549_99.3%
HCC515_98.7%
VCAP_96.3%
HEPG2_90.4%
HELA_47.9%
YAPC_47.9%
U937_12.5%
LOVO_12.4%
SNUC4_12.4%
SKMEL1_12.4%
RMUGS_12.4%
HCC15_12.4%
HEC108_12.4%
CORL23_12.4%
A673_12.4%
NCIH596_12.3%
TYKNU_12.3%
SW948_12.3%
SW620_12.3%
SNU1040_12.3%

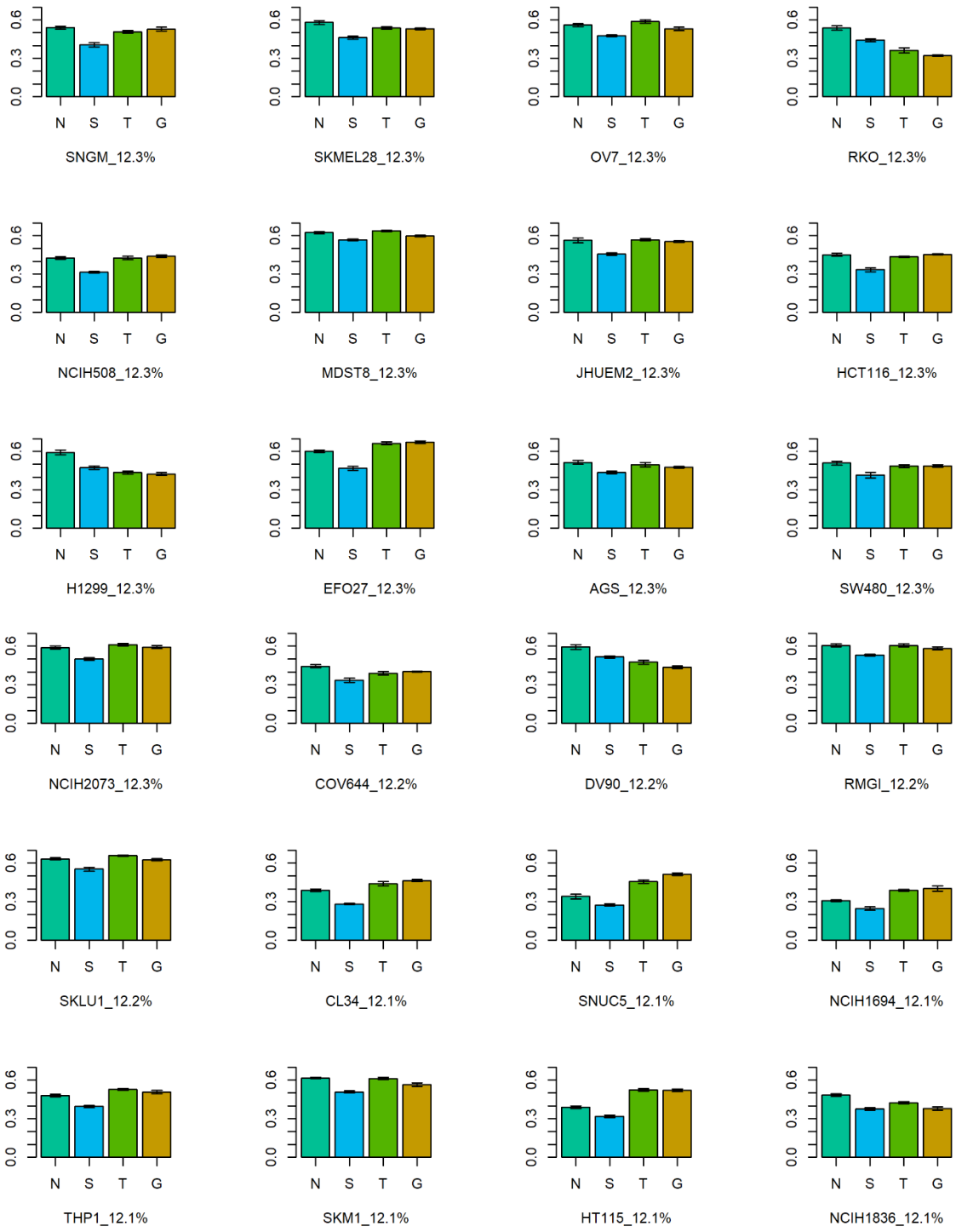
0.0 0.3 0.6
N S T G
SNGM_12.3%
SKMEL28_12.3%
OV7_12.3%
RKO_12.3%
NCIH508_12.3%
MDST8_12.3%
JHUEM2_12.3%
HCT116_12.3%
H1299_12.3%
EFO27_12.3%
AGS_12.3%
SW480_12.3%
NCIH2073_12.3%
COV644_12.2%
DV90_12.2%
RMGI_12.2%
SKLU1_12.2%
CL34_12.1%
SNUC5_12.1%
NCIH1694_12.1%
THP1_12.1%
SKM1_12.1%
HT115_12.1%
NCIH1836_12.1%

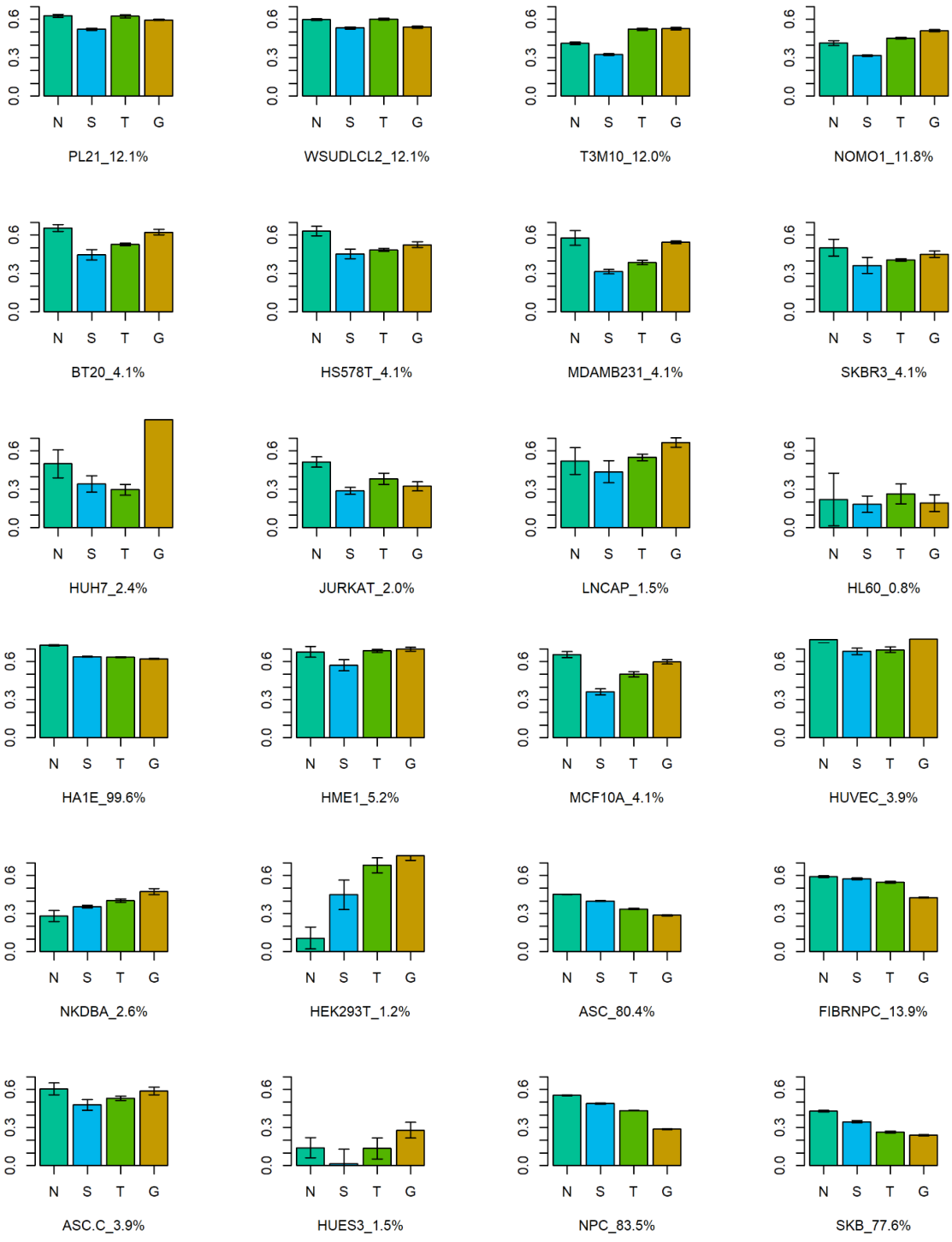
0.0 0.3 0.6
N S T G
PL21_12.1%
WSUDLCL2_12.1%
T3M10_12.0%
NOMO1_11.8%
BT20_4.1%
HS578T_4.1%
MDAMB231_4.1%
SKBR3_4.1%
HUH7_2.4%
JURKAT_2.0%
LNCAP_1.5%
HL60_0.8%
HA1E_99.6%
HME1_5.2%
MCF10A_4.1%
HUVEC_3.9%
NKDBA_2.6%
HEK293T_1.2%
ASC_80.4%
FIBRNPC_13.9%
ASC.C_3.9%
HUES3_1.5%
NPC_83.5%
SKB_77.6%

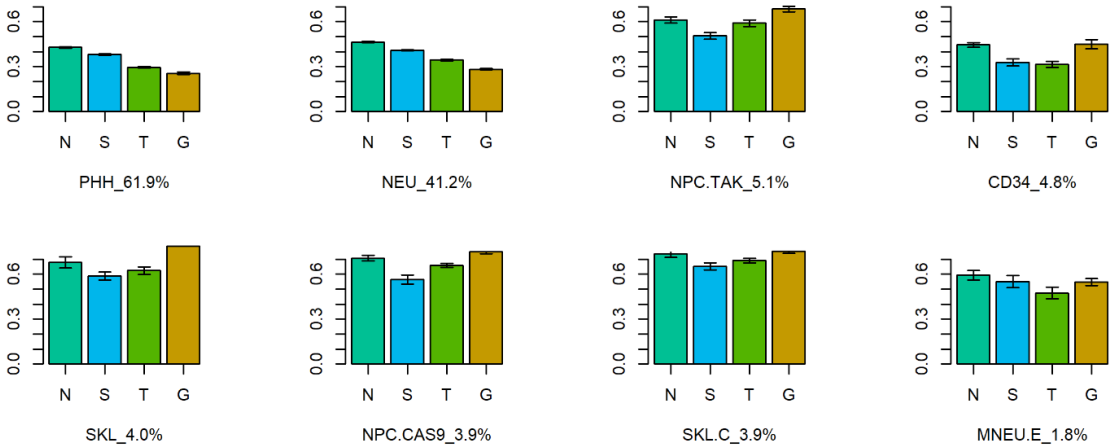

Figure 1: Positive weighted connectivity correlation across all genes and drugs, for each of the 80 cell lines in the sparse matrix. Methods are denoted by single-letter labels: N : neighborhood collaborative approach; S : SVD; T : two-way average; G : tissue-aGnostic (baseline method). Organized by cell type (cancer, immortalized, stem and primary) and ordered by percentage of drugs profiled in each cell. Error bars show variation across cross validation runs.

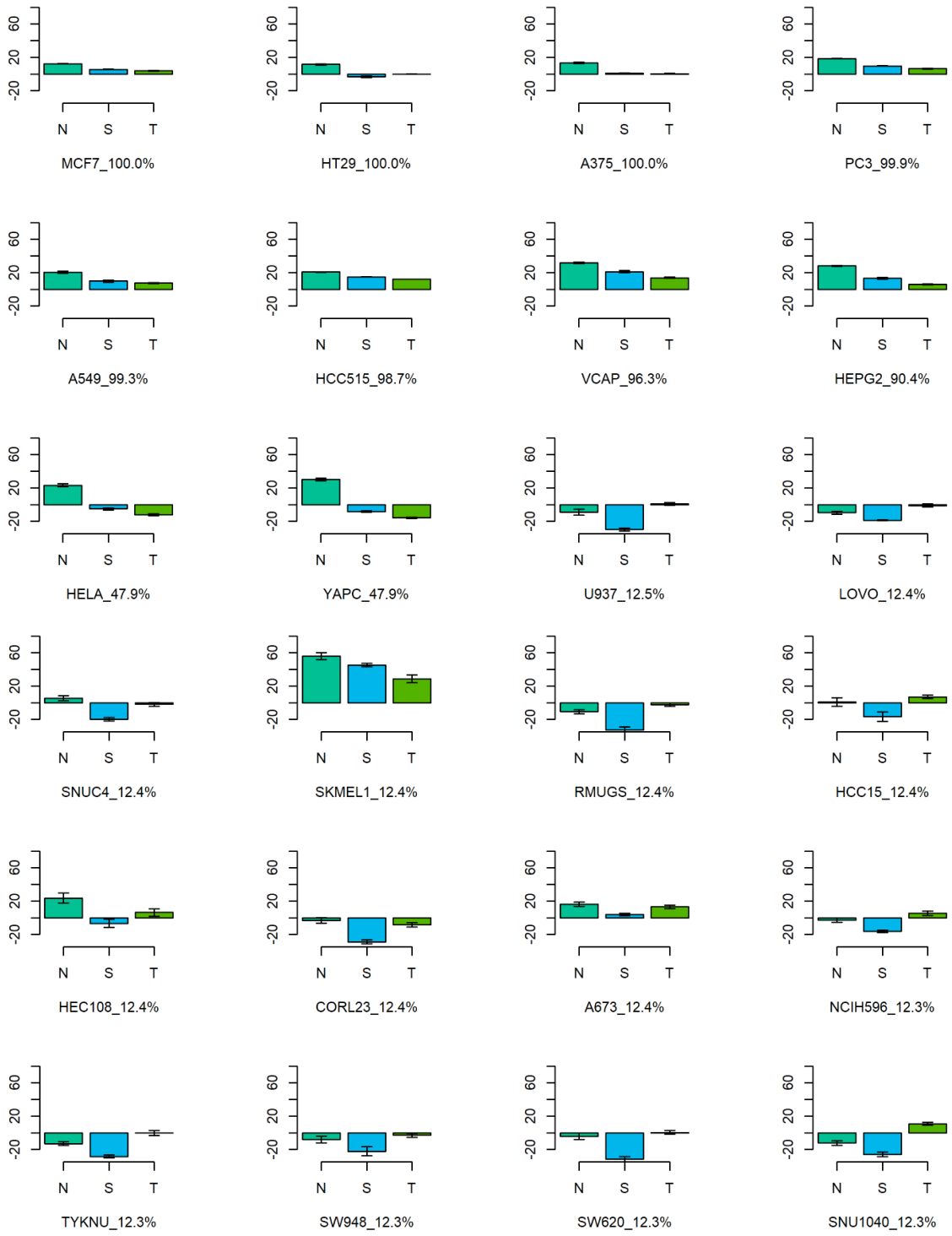
-20
20
60
N
S
T
MCF7_100.0%
HT29_100.0%
A375_100.0%
PC3_99.9%
A549_99.3%
HCC515_98.7%
VCAP_96.3%
HEPG2_90.4%
HELA_47.9%
YAPC_47.9%
U937_12.5%
LOVO_12.4%
SNUC4_12.4%
SKMEL1_12.4%
RMUGS_12.4%
HCC15_12.4%
HEC108_12.4%
CORL23_12.4%
A673_12.4%
NCIH596_12.3%
TYKNU_12.3%
SW948_12.3%
SW620_12.3%
SNU1040_12.3%

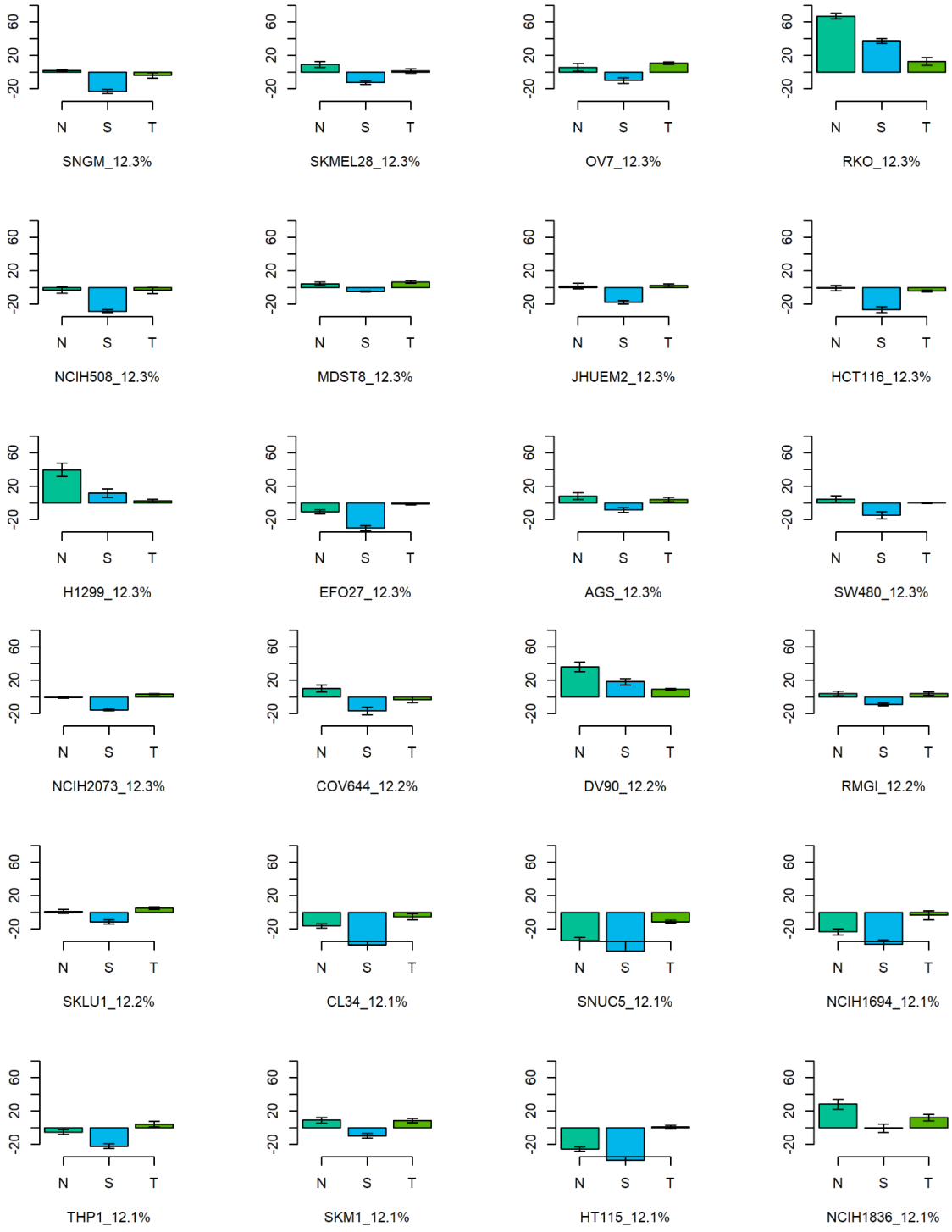
-20
20
60
N
S
T
SNGM_12.3%
SKMEL28_12.3%
OV7_12.3%
RKO_12.3%
NCIH508_12.3%
MDST8_12.3%
JHUEM2_12.3%
HCT116_12.3%
H1299_12.3%
EFO27_12.3%
AGS_12.3%
SW480_12.3%
NCIH2073_12.3%
COV644_12.2%
DV90_12.2%
RMGI_12.2%
SKLU1_12.2%
CL34_12.1%
SNUC5_12.1%
NCIH1694_12.1%
THP1_12.1%
SKM1_12.1%
HT115_12.1%
NCIH1836_12.1%

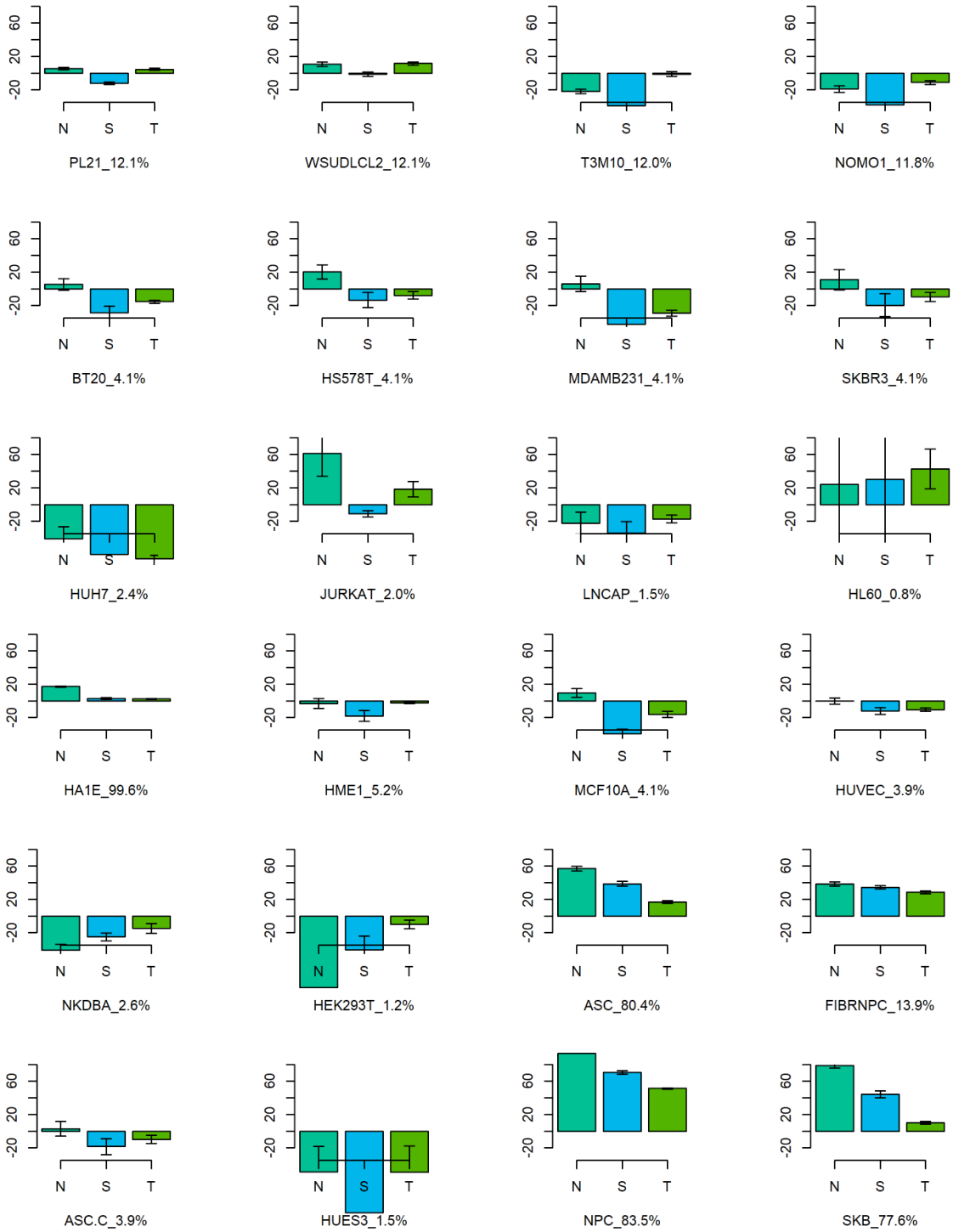
-20
20
60
N
S
T
PL21_12.1%
WSUDLCL2_12.1%
T3M10_12.0%
NOMO1_11.8%
BT20_4.1%
HS578T_4.1%
MDAMB231_4.1%
SKBR3_4.1%
HUH7_2.4%
JURKAT_2.0%
LNCAP_1.5%
HL60_0.8%
HA1E_99.6%
HME1_5.2%
MCF10A_4.1%
HUVEC_3.9%
NKDBA_2.6%
HEK293T_1.2%
ASC_80.4%
FIBRNPC_13.9%
ASC.C_3.9%
HUES3_1.5%
NPC_83.5%
SKB_77.6%

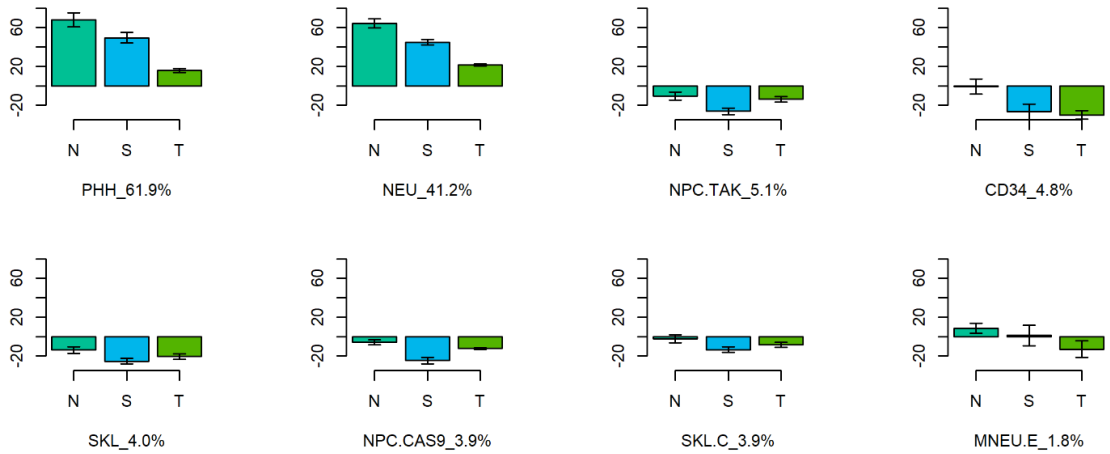

Figure 2: Percent change in positive weighted connectivity correlation compared to the tissue-agnostic method. Methods are denoted by single-letter labels: N : neighborhood collaborative approach; S : SVD; T : two-way average; G : tissue-aGnostic (baseline method). Organized by cell type (cancer, immortalized, stem and primary) and ordered by percentage of drugs profiled in each cell. Error bars show variation across cross validation runs.

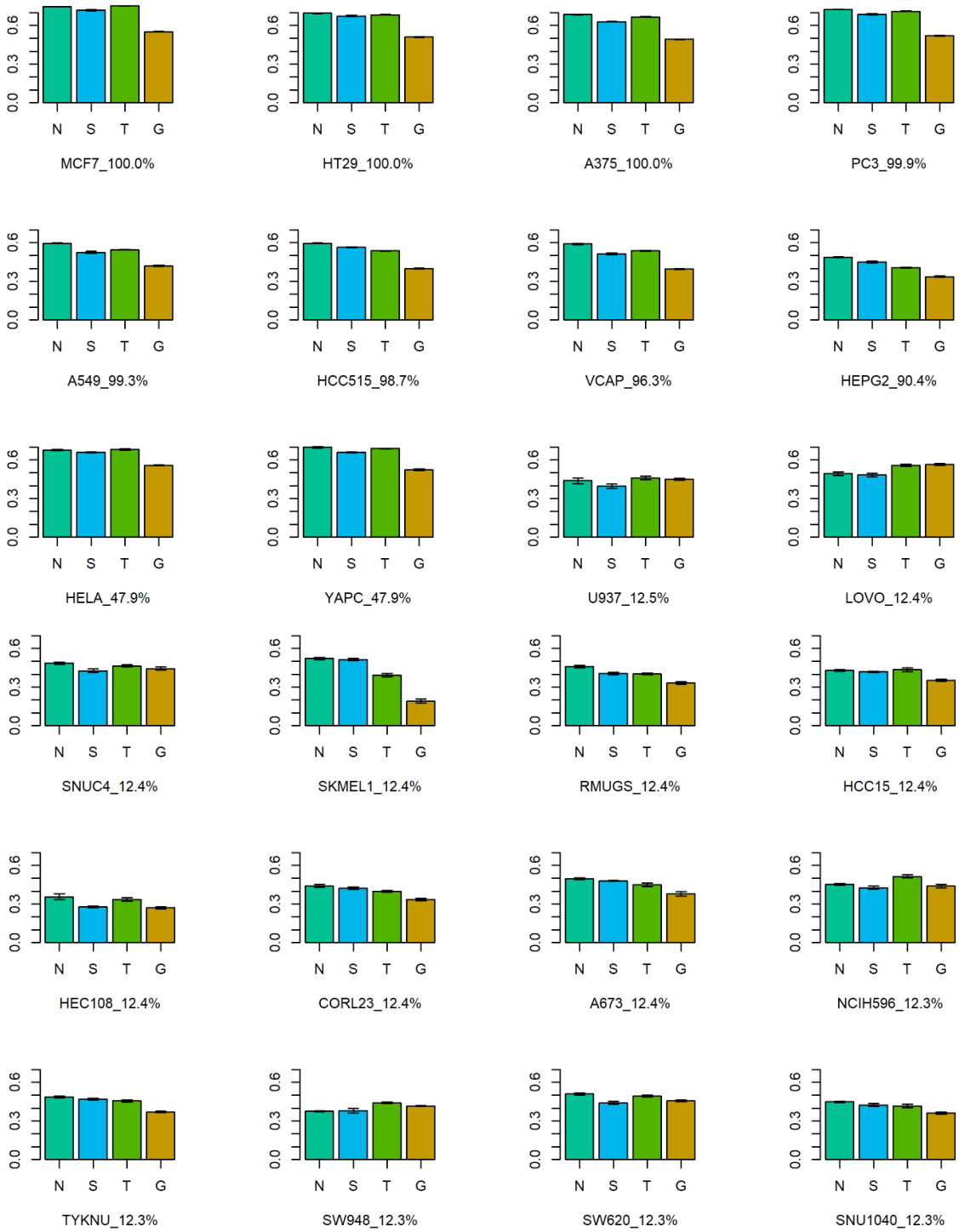
0.0 0.3 0.6
N S T G
MCF7_100.0%
HT29_100.0%
A375_100.0%
PC3_99.9%
A549_99.3%
HCC515_98.7%
VCAP_96.3%
HEPG2_90.4%
HELA_47.9%
YAPC_47.9%
U937_12.5%
LOVO_12.4%
SNUC4_12.4%
SKMEL1_12.4%
RMUGS_12.4%
HCC15_12.4%
HEC108_12.4%
CORL23_12.4%
A673_12.4%
NCIH596_12.3%
TYKNU_12.3%
SW948_12.3%
SW620_12.3%
SNU1040_12.3%

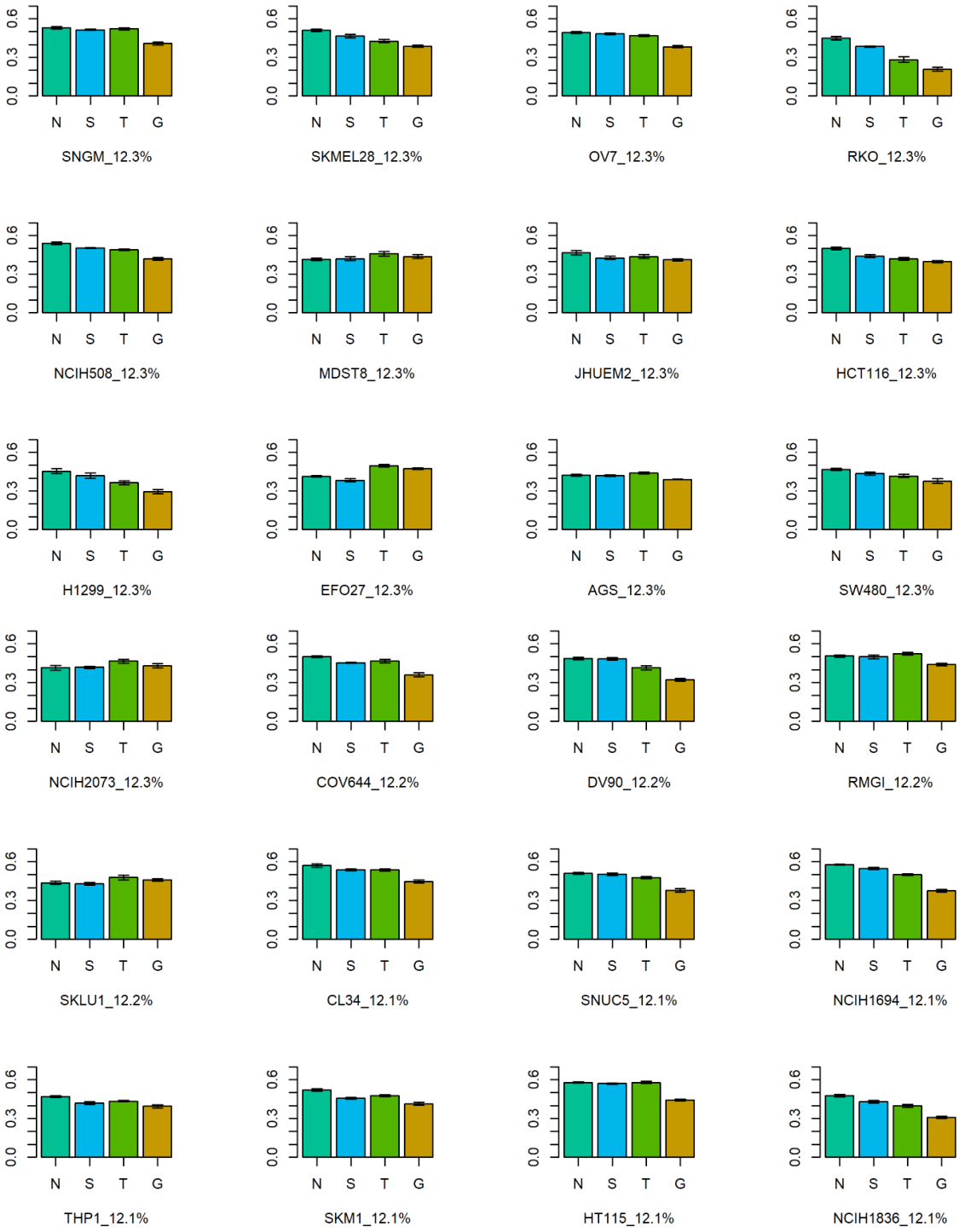
0.0 0.3 0.6
N S T G
SNGM_12.3%
SKMEL28_12.3%
OV7_12.3%
RKO_12.3%
NCIH508_12.3%
MDST8_12.3%
JHUEM2_12.3%
HCT116_12.3%
H1299_12.3%
EFO27_12.3%
AGS_12.3%
SW480_12.3%
NCIH2073_12.3%
COV644_12.2%
DV90_12.2%
RMGI_12.2%
SKLU1_12.2%
CL34_12.1%
SNUC5_12.1%
NCIH1694_12.1%
THP1_12.1%
SKM1_12.1%
HT115_12.1%
NCIH1836_12.1%

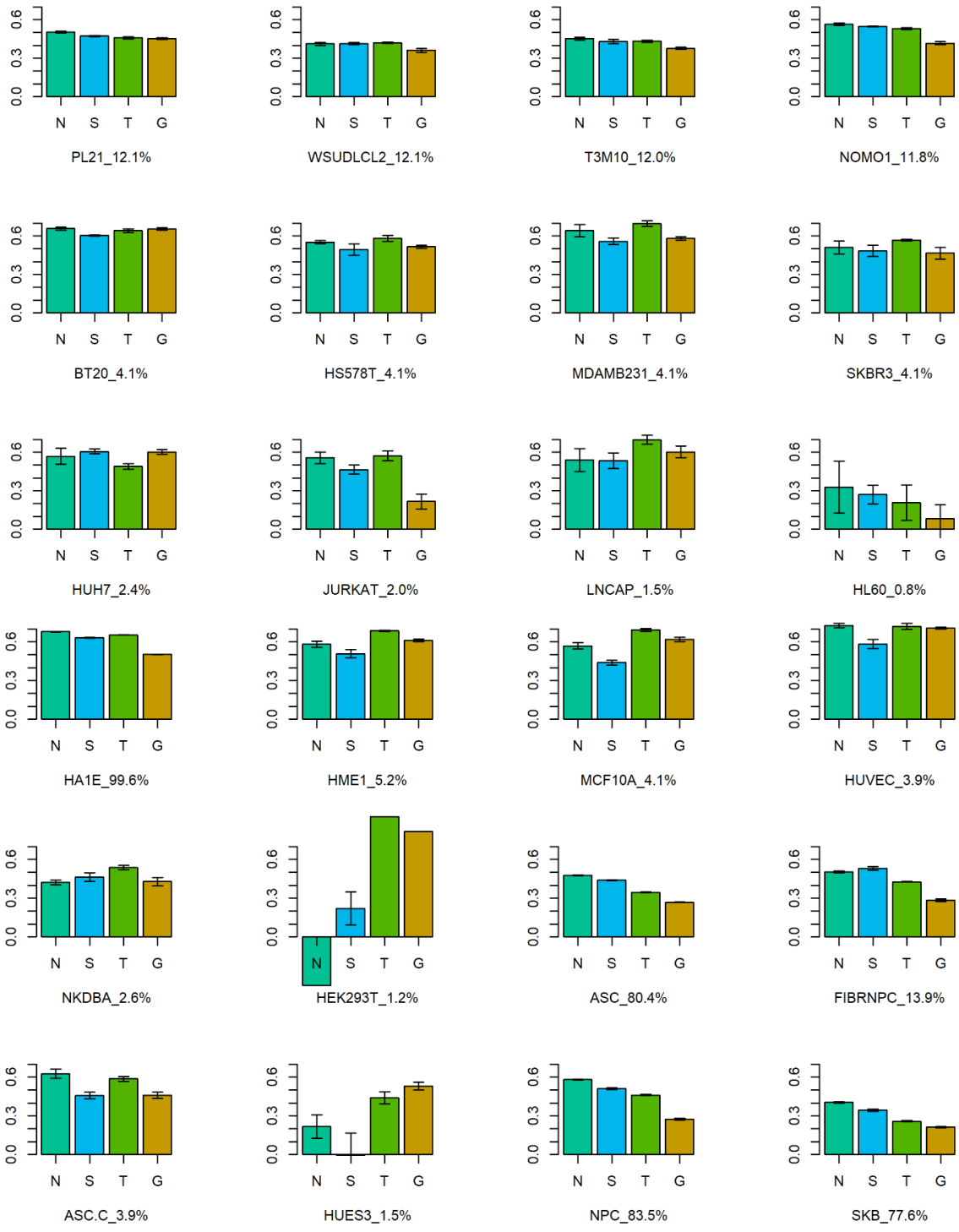
0.0 0.3 0.6
N S T G
PL21_12.1%
WSUDLCL2_12.1%
T3M10_12.0%
NOMO1_11.8%
BT20_4.1%
HS578T_4.1%
MDAMB231_4.1%
SKBR3_4.1%
HUH7_2.4%
JURKAT_2.0%
LNCAP_1.5%
HL60_0.8%
HA1E_99.6%
HME1_5.2%
MCF10A_4.1%
HUVEC_3.9%
NKDBA_2.6%
HEK293T_1.2%
ASC_80.4%
FIBRNPC_13.9%
ASC.C_3.9%
HUES3_1.5%
NPC_83.5%
SKB_77.6%

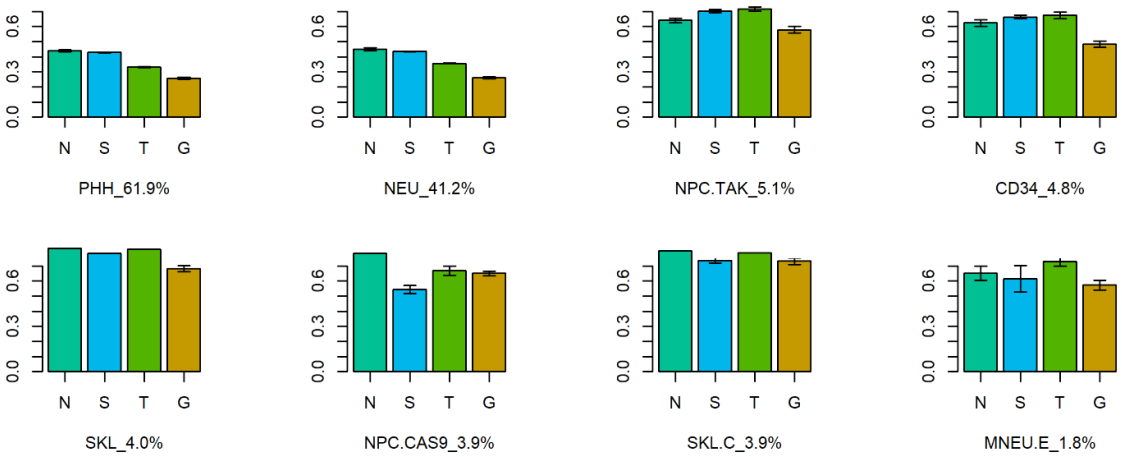

Figure 3: Negative weighted connectivity correlation across all genes and drugs, for each of the 80 cell lines in the sparse matrix. Methods are denoted by single-letter labels: N : neighborhood collaborative approach; S : SVD; T : two-way average; G : tissue-aGnostic (baseline method). Organized by cell type (cancer, immortalized, stem and primary) and ordered by percentage of drugs profiled in each cell. Error bars show variation across cross validation runs.

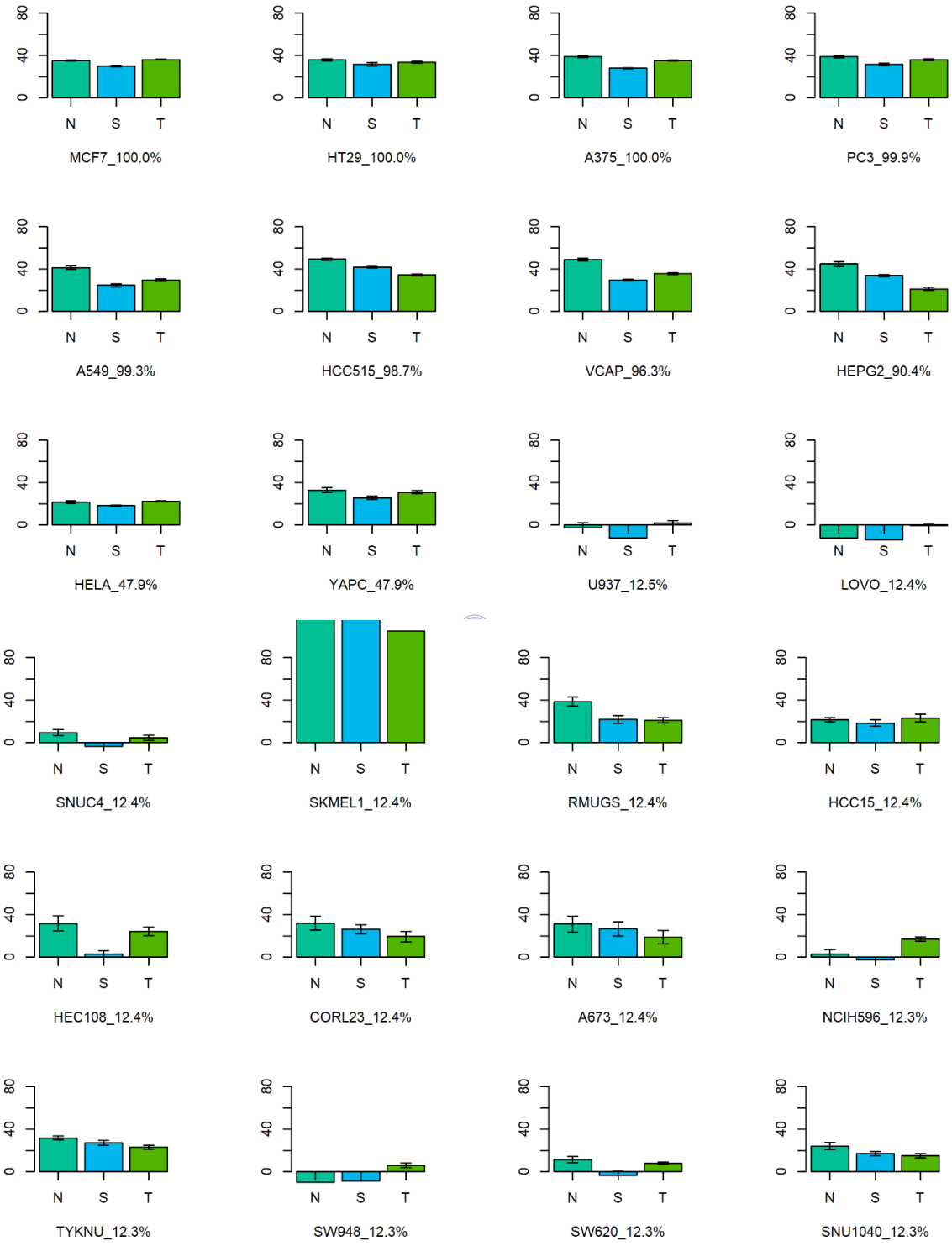
0
40
80
N
S
T
MCF7_100.0%
HT29_100.0%
A375_100.0%
PC3_99.9%
A549_99.3%
HCC515_98.7%
VCAP_96.3%
HEPG2_90.4%
HELA_47.9%
YAPC_47.9%
U937_12.5%
LOVO_12.4%
SNUC4_12.4%
SKMEL1_12.4%
RMUGS_12.4%
HCC15_12.4%
HEC108_12.4%
CORL23_12.4%
A673_12.4%
NCIH596_12.3%
TYKNU_12.3%
SW948_12.3%
SW620_12.3%
SNU1040_12.3%

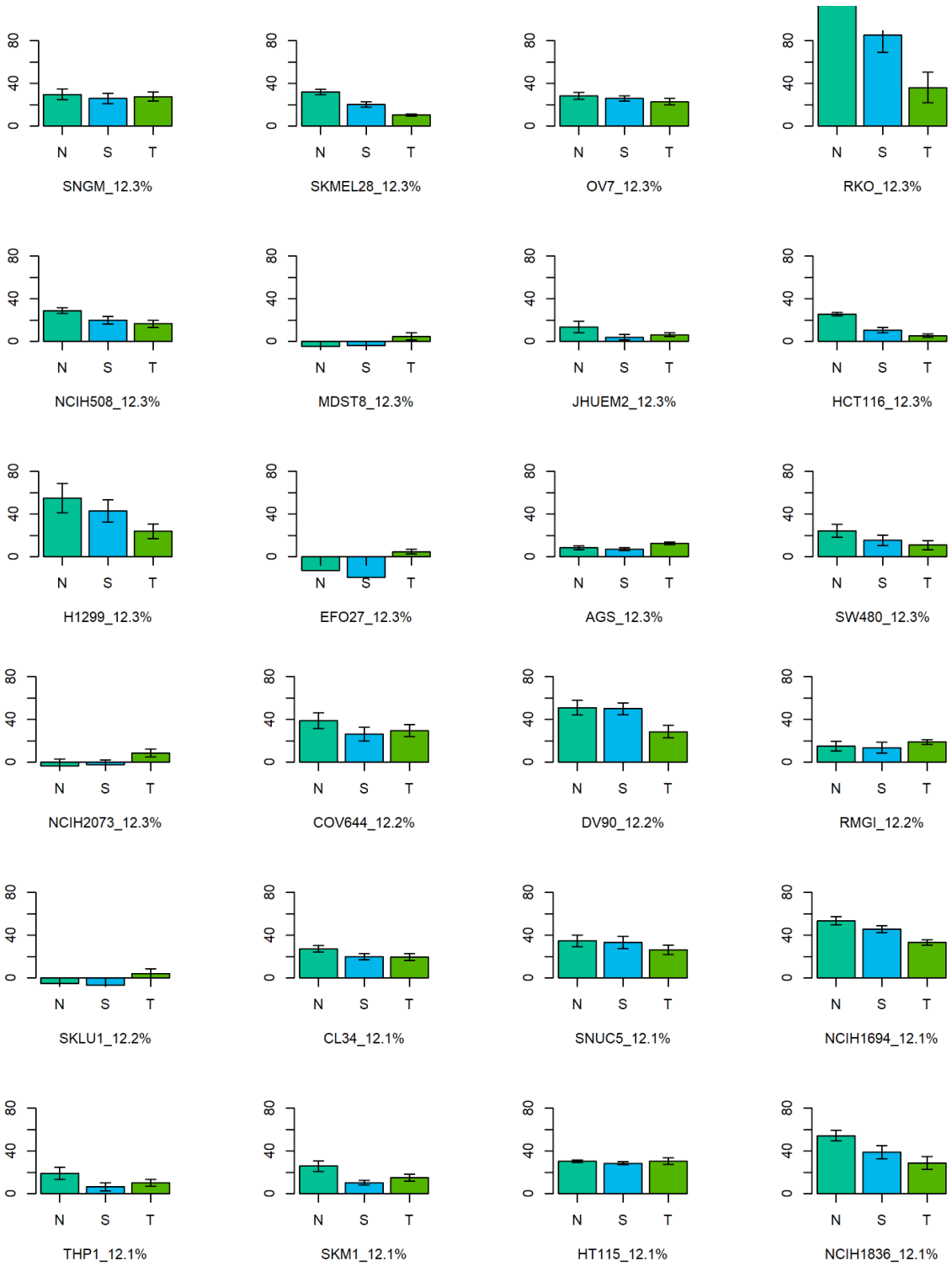
0
40
80
N
S
T
SNGM_12.3%
SKMEL28_12.3%
OV7_12.3%
RKO_12.3%
NCIH508_12.3%
MDST8_12.3%
JHUEM2_12.3%
HCT116_12.3%
H1299_12.3%
EFO27_12.3%
AGS_12.3%
SW480_12.3%
NCIH2073_12.3%
COV644_12.2%
DV90_12.2%
RMGI_12.2%
SKLU1_12.2%
CL34_12.1%
SNUC5_12.1%
NCIH1694_12.1%
THP1_12.1%
SKM1_12.1%
HT115_12.1%
NCIH1836_12.1%

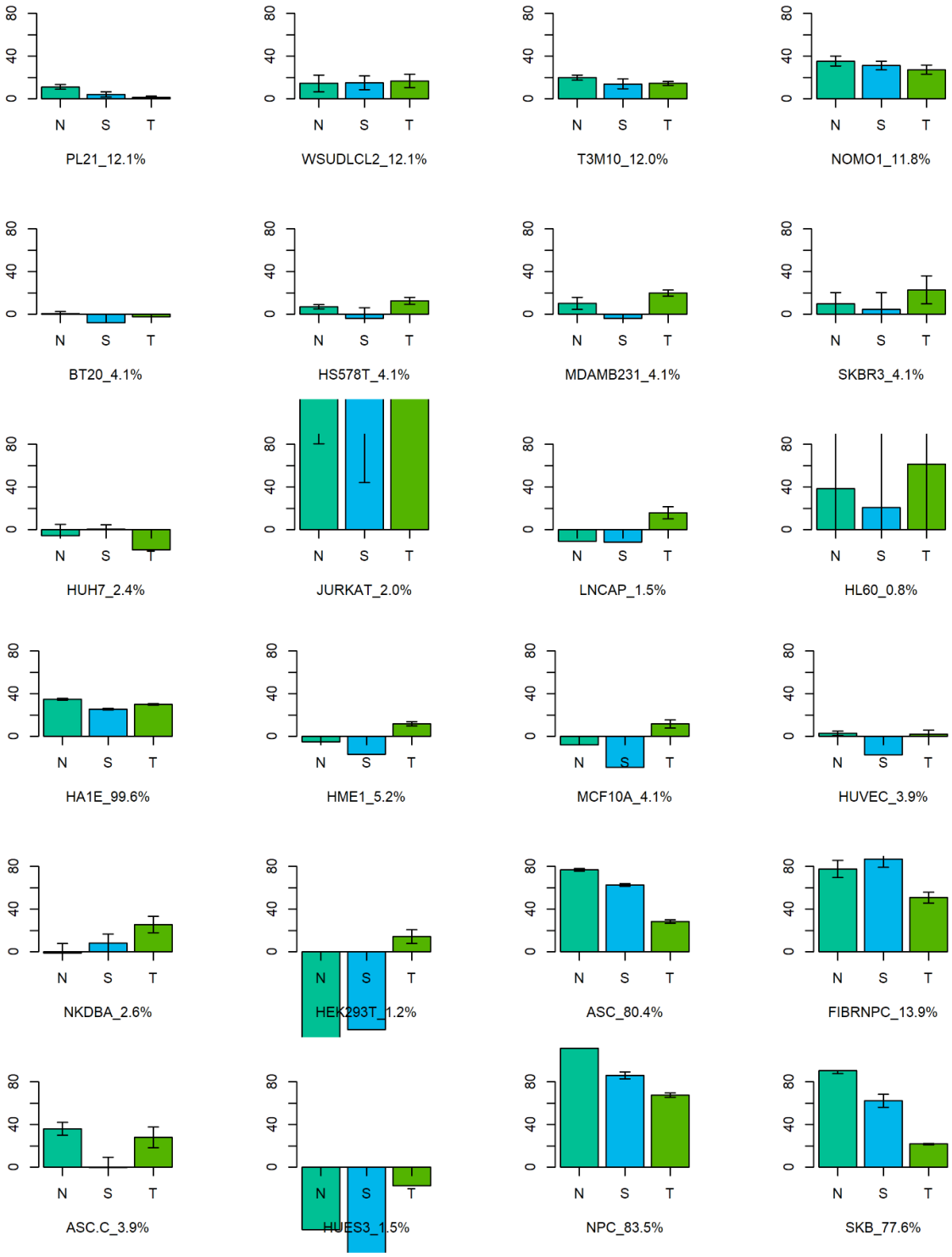
0
40
80
N
S
T
PL21_12.1%
WSUDLCL2_12.1%
T3M10_12.0%
NOMO1_11.8%
BT20_4.1%
HS578T_4.1%
MDAMB231_4.1%
SKBR3_4.1%
HUH7_2.4%
JURKAT_2.0%
LNCAP_1.5%
HL60_0.8%
HA1E_99.6%
HME1_5.2%
MCF10A_4.1%
HUVEC_3.9%
NKDBA_2.6%
HEK293T_1.2%
ASC_80.4%
FIBRNPC_13.9%
ASC.C_3.9%
HUES3_1.5%
NPC_83.5%
SKB_77.6%

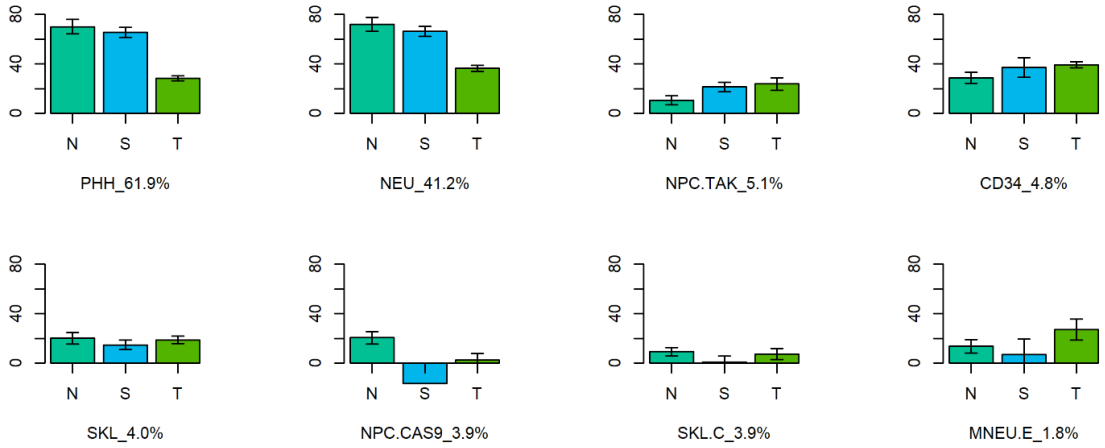

Figure 4: Percent change in negative weighted connectivity correlation compared to the tissue-agnostic method. Methods are denoted by single-letter labels: N : neighborhood collaborative approach; S : SVD; T : two-way average; G : tissue-aGnostic (baseline method). Organized by cell type (cancer, immortalized, stem and primary) and ordered by percentage of drugs profiled in each cell. Error bars show variation across cross validation runs.

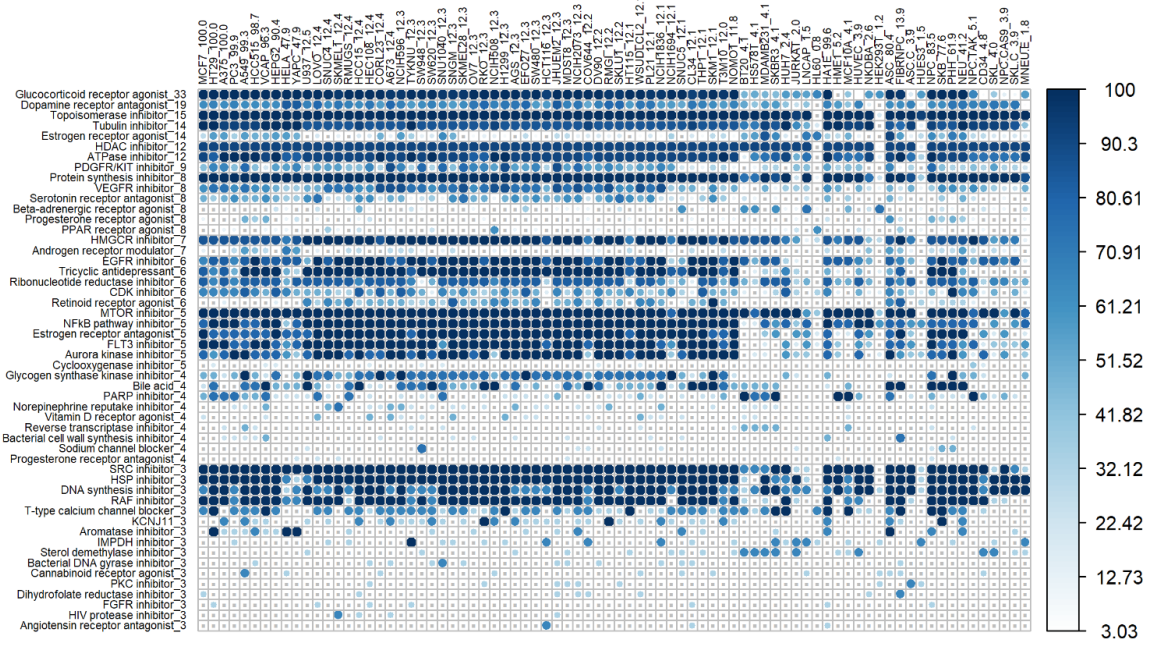

Figure 5: Percent of drugs correctly expressing strong connectivity to their drug class using the fully imputed sparse matrix by the neighborhood approach. Cells are organized by cell type (cancer, immortalized, stem and primary) and ordered by percentage of drugs profiled in each cell. PCL sets are ordered by the number of drugs in each set that are in the sparse matrix. The darker the shade of blue, the higher percentage of drugs with statistically significant NES scores. Grey dots represent PCL/cell combinations in which there were no statistically significant NES scores. In the main text, primary cells were pulled out and the plot was transposed for readability.

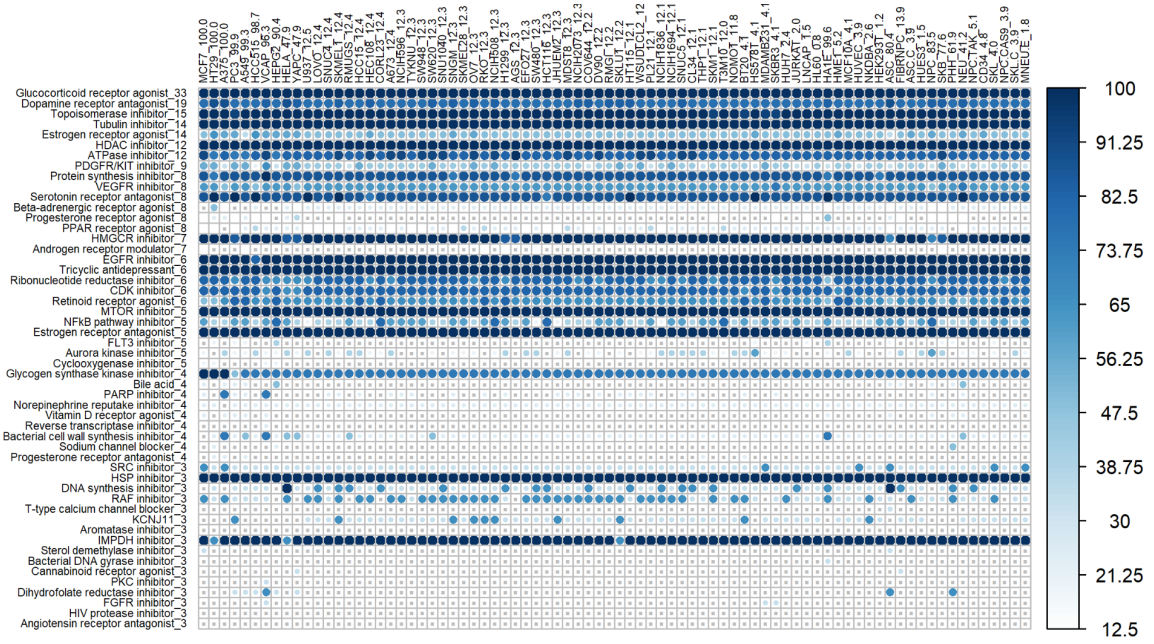

Figure 6: Percent of drugs correctly expressing strong connectivity to their drug class using the fully imputed sparse matrix by the tissue agnostic approach. Cells are organized by cell type (cancer, immortalized, stem and primary) and ordered by percentage of drugs profiled in each cell. PCL sets are ordered by the number of drugs in each set that are in the sparse matrix. The darker the shade of blue, the higher percentage of drugs with statistically significant NES scores. Grey dots represent PCL/cell combinations in which there were no statistically significant NES scores. In the main text, primary cells were pulled out and the plot was transposed for readability.

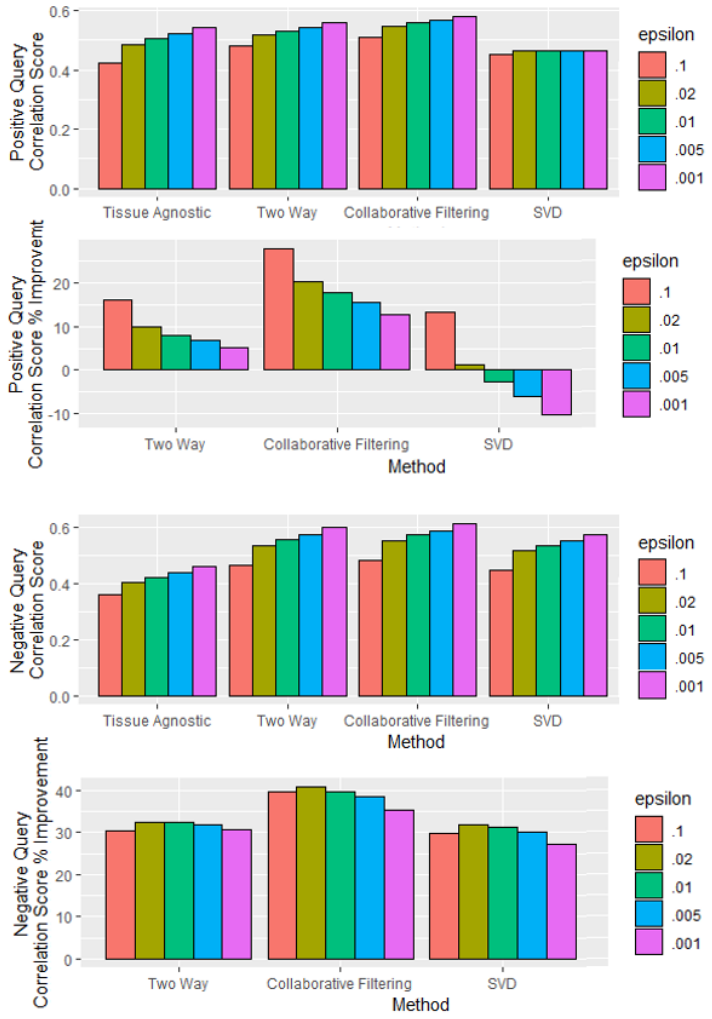

Figure 7: Change in average positive and negative query correlation scores across all cells and drugs obtained by varying ϵ by a factor of either two or ten in either direction from the values of $\epsilon = .01$ used in this work.

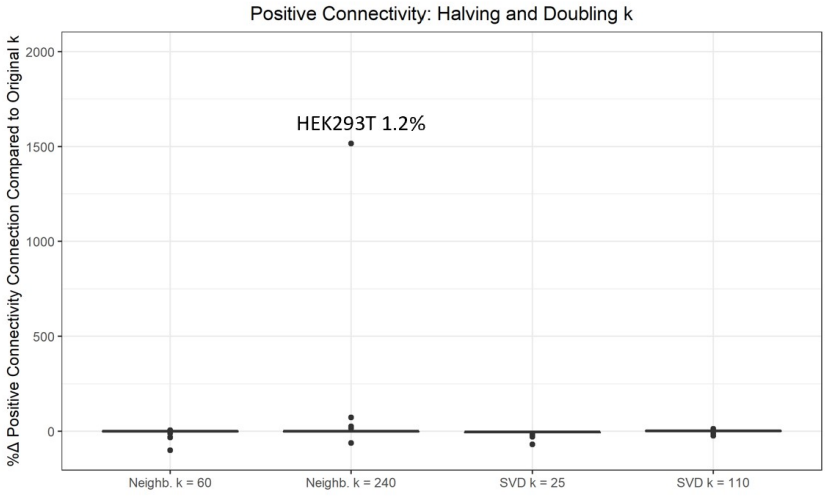

Figure 8: Percent change in average positive weighted connectivity correlation across all drugs and genes obtained by varying k by a factor of two from the values of $k = 120$ for nearest neighbors and $k = 55$ for svd used in this work for the sparse data set. Outlier cell lines labelled with %data.

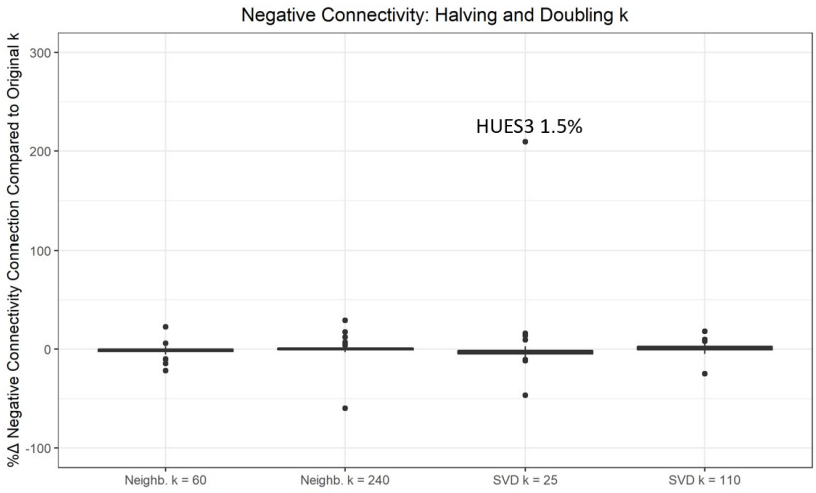

Figure 9: Percent change in average negative weighted connectivity correlation across all drugs and genes obtained by varying k by a factor of two from the values of $k = 120$ for nearest neighbors and $k = 55$ for svd used in this work for the sparse data set. Outlier cell lines labelled with %data.